Size disparity and lower critical solution temperature: A critical investigation of free-volume disparity

Mukesh Chhajer and P. D. Gujrati

Citation: The Journal of Chemical Physics **109**, 9022 (1998); doi: 10.1063/1.477573
View online: http://dx.doi.org/10.1063/1.477573
View Table of Contents: http://scitation.aip.org/content/aip/journal/jcp/109/20?ver=pdfcov
Published by the AIP Publishing

Size disparity and lower critical solution temperature: A critical investigation of free-volume disparity

Mukesh Chhajer
Department of Polymer Science, and Maurice Morton Institute of Polymer Science, The University of Akron, Akron, Ohio 44325

P. D. Gujrati[a)]
Department of Physics and Department of Polymer Science, and Maurice Morton Institute of Polymer Science, The University of Akron, Akron, Ohio 44325

(Received 18 March 1998; accepted 19 August 1998)

By critically examining a simple model system of equilibrium polymerization that is athermal in the traditional sense, we demonstrate that many of the consequences of the free-volume disparity induced by size disparity are inconsistent with its current understanding. Despite its traditional name, the model is not truly athermal because of the compressibility. The resulting energetics endows the model system with a very rich and complex behavior. The analytical results that are obtained in a mean-field approximation show how and when an upper critical solution temperature, a lower critical solution temperature (LCST) and an immiscibility loop may occur. We suggest that it is the difference in the thermal volume-expansion coefficients rather than the difference in free volumes of the coexisting phases (and not of the components) that plays a central role in determining the phenomenon of LCST and may be used to provide for its quantitative characterization. Too much or too little of free volume disfavors LCST; hence, it occurs only in a finite range of the pressure. Moreover, for the phenomenon of LCST to occur, the size disparity should be larger than some critical value that also depends on the pressure. A line of theta points is found in a four-parameter phase space characterizing the simple model. The model also enables us to understand how a variety of phase diagrams including hourglass emerges, despite the fact that the conventional mechanism for hourglass in not present. © *1998 American Institute of Physics.* [S0021-9606(98)50944-0]

I. INTRODUCTION

Polymer compatibility[1] plays an important role in the technological applications of polymers. Subtle changes in the free energy of mixing may be sufficient to change a miscible mixture into an immiscible mixture as the temperature is raised. This gives rise to the existence of a lower critical solution temperature (LCST) as first observed by Freeman and Rowlinson[2] in addition to the phenomenon of an upper critical solution temperature (UCST). In view of the small driving forces required for thermally induced phase separation, a complete thermodynamic understanding of the phenomenon is vital not only from an experimental, but also from a theoretical point of view. It is widely believed[3–9] that the interesting phenomenon of LCST in a *binary mixture* is due to the ''*free-volume dissimilarity or disparity*'' associated with molecular size disparity, as first proposed by Mathot, Prigogine and Trappeniers,[3–5] a condition readily fulfilled in most polymer solutions and blends. In particular, the phenomenon of LCST is usually observed in simple fluids with *strong polar interaction*, e.g., in aqueous solutions. However, it is found to exist, as a rule rather than as an exception, in most polymer solutions, even though they are weakly interacting, presumably because of the above-mentioned *size disparity* between long polymers and small solvent molecules. In most cases, the value of LCST lies within a range of 10%–30% below the critical temperature for the pure solvent.

As temperature rises, the free-volume disparity between molecules increases and favors demixing.[3–9] This is to contrast with the old proverb ''like dissolves like.''[7] The concept of free volume has been an intriguing one that permeates throughout physics but is not well understood, at least in our opinion. Consequently, it has not been put in any *quantitative* and *rational* form based on first principles. The closest we have come is the general discussion in Ref. 8, the *quantitative* predictions of which are mostly in accordance with the *qualitative* predictions of Patterson.[7] There still remains major gaps in our conceptual understanding of free volume, a concept whose veracity has not been checked based on first principles. Thus, it is desirable to take a critical look at it from a basic point of view. It is this desire that has motivated the present study.

The adimensional effective chi parameter $\tilde{\chi}$ [defined as the half of the left-hand-side of the inequality, Eq. (58b) in Ref. 8] is a sum of two contributions χ_1 and χ_2 that behave differently as functions of the temperature T (measured in the units of the Boltzmann constant). The first contribution χ_1 is *energetic* in origin and is a monotonically decreasing function of T. The second contribution has its origin in the *free volume* and is either a monotonically increasing function

a)Electronic mail: pdg@arjun.physics.uakron.edu

or can have a hump followed by a monotonically increasing part as T is increased. In the latter case, χ_2 has a zero at a temperature T_0, see Eq. (64) in Ref. 8, which may be less than the spinodal temperature T_s at which χ_2 diverges. The divergence at the spinodal plays an important role in the analysis.[8] Both contributions are positive whenever there is an effective repulsion between the two mixing components.[7,8]

Consider the simple case when the volumes per monomer of the mixing species are *identical*. For a symmetric blend, for example, for which there is no size disparity, χ_2 must vanish as both species have identical free-volume effects. Indeed, such a situation commonly arises in computer simulations in which one can easily include an effective interaction between the two symmetric species; see for example, Ref. 10. For such systems, the phenomenon of LCST must be absent. On the other hand, the contribution χ_2 does not generally vanish for a symmetric blend.[8] Even for an asymmetric blend, Lacombe and Sanchez[8] suggest that LCST will exist for *all* pressures, low or high. This is perplexing since one does not expect to observe any LCST at extremely high pressures as *no* LCST exists in the incompressible limit. Therefore, the concept of ''free-volume disparity'' due to size disparity alone is still not a well-understood concept.

To the best of our knowledge, there has been *no* significant attempt to obtain a quantitative measure of the free-volume disparity even though the concept itself is trivial to introduce: it represents ''the dissimilarity between the free volumes of the'' mixing components, to quote Patterson.[7] But the free volumes in the pure states of the mixing components, though useful in their own right, are going to be *different* at *all* temperatures and pressures because of the size disparity alone, whether the mixture is miscible or not. They also do not contain the important contributions from *energetics* during mixing. To incorporate this additional effect, we *suggest* that it is useful to consider, as a *measure* of the free-volume disparity, the *difference* between the free volumes of the two *coexisting* phases in the mixture and investigate its behavior as a function of temperature and its relationship with the phenomenon of LCST. Indeed, we find that the *volume-expansion coefficient* is the most important quantity to investigate.

In order to investigate *only* the effect of size disparity on free volume, we consider a very simple system in which there is *no* effective interaction energy between the two components. This ensures that the energetic contribution χ_1 to the ''effective chi'' vanishes in the system and that the *entire physics* is determined by size-disparity induced free-volume effects. The model is simple enough so that a thorough analytical investigation is possible, as we show. This allows us to provide a critical evaluation of and some analytical justification for the importance of the free-volume concept.

The importance of such a model system was already advocated by Patterson[7] to study the effects of free-volume disparity. A very simple but realistic *example* is obtained by considering a compressible model of equilibrium polymerization in which unreacted monomers play the role of the solvent. We will call the reacted (unreacted) monomers the segments (the solvent molecules) in the following. Since the segments and the solvent molecules are homologous, the effective interaction energy ε between them vanishes and we have, what is customarily described in the literature as, an *athermal* mixture. For such a choice of the energies, the Flory–Huggins chi parameter $\chi=0$ and $T_0=0$, (see Ref. 8). Since $T_0=0$, χ_2 must be a monotonically increasing function of T between $T=0$ and $T=T_s$. For this particular simple system, some of the consequences of our current understanding are as follows:

(i) LCST exists for all sizes as long as they are different for the two species,
(ii) LCST exists at all pressures,
(iii) LCST $\leqslant T_s$,
(iv) UCST cannot exist by itself (since χ_1 is zero), and
(v) an hourglass effect cannot emerge (as there is no UCST in the model for the LCST to merge with).

We will show below that we cannot substantiate these observations in our analytical approach, which offers a most comprehensive analysis of free-volume effects to date.

The layout of the paper is as follows. We introduce the simple ''athermal'' model in Sec. II. We argue that despite its traditional nomenclature, it is far from being an athermal system. Various limiting cases of this model are discussed there. We use previously known results and heuristic arguments to reveal the possible phases in the model. In Sec. III, we introduce a magnetic analogy which possesses certain *symmetry* properties that are quite useful in analyzing the phase diagram. The magnetic model is solved in a mean-field approximation in Sec. IV. The phase diagram is thoroughly investigated in Sec. V, both analytically and numerically. This is the most important part of the paper, where we constantly switch back and forth between the magnetic picture and the polymer picture. We warn that the analysis at places becomes too complicated and requires patience on the part of the reader. A reader who does not wish to follow the magnetic analogy and the technical details of the mean-field solution may skip Secs. IV and V and go directly to Sec. VI. This section contains an elaborate discussion of the physics of the model and a summary of the work.

II. ''ATHERMAL'' MODEL SYSTEM

We consider a compressible model of equilibrium polymerization on a regular lattice of coordination number q and the total number of sites N; $N\to\infty$ for the thermodynamic limit which will be always understood in the following. The monomers polymerize to form polydisperse polymers. The compressibility is accounted for by introducing voids[11] on the lattice, such that each site of the lattice is either occupied by a void or by a monomer. As said earlier, we will use an index j to represent the three species in the model: $j=0$ represents voids, $j=1$ represents the segment and $j=2$ represents the solvent. Since the solvent and the polymer segments are chemically identical, there is *no* effective interaction, specific or otherwise, between them. This is because, on a regular lattice, what counts is the effective interaction ε_{ij} between two species:[12,13]

$$\varepsilon_{ij}=e_{ij}-(e_{ii}+e_{jj})/2,$$

where e_{ij} denotes the ''bare'' van der Waals interaction energies between the two species i and j. Since $j=1$ and $j=2$ are homologous, $e=e_{11}=e_{22}=e_{12}$. Hence, $\varepsilon_{12}=0$ and the corresponding chi parameter $\chi=\beta q\varepsilon_{12}=0$, where β is the inverse temperature T. The above relation between ε_{ij} and e_{ij}'s is a direct consequence of the geometrical relations among quantities of interest imposed by the homogeneous lattice structure, see Eqs. (2.3)–(2.4) in Ref. 12.

The fact that $\varepsilon_{12}=0$ has been used to imply that such a solution is *athermal*. This is *not* a correct view. On a lattice, the above solution must be described by three independent effective interaction energies: ε_{01}, ε_{02} and ε_{12}. While $\varepsilon_{12}=0$, the other remaining energies are, in general, nonzero and equal

$$\varepsilon\equiv\varepsilon_{01}=\varepsilon_{02}=-e/2,$$

where we have used the physical observation that $e_{00}=e_{01}=e_{02}=0$ as voids do not interact either among themselves or with other monomers. Because of the energetics, the model is *not* truly athermal. It is easily seen that this choice also ensures that $T_0=0$.

The above situation naturally arises in the above-mentioned equilibrium polymerization process. Such a polydisperse system is ideal for our analytical work as explained below. However, the results obtained here are expected to be applicable even for a system of monodisperse polymers, as will also be discussed later in Sec. VI. The polydisperse polymeric species $j=1$ requires two activities κ, the activity for forming a bond to control the average length of polymers, and η, the activity for an end point of a polymer to control their number, respectively. Similarly, we need an activity λ, the activity for a monomer to control the number of all monomers, reacted or not. Even though the general model system would require three different energies, the above simple system requires only one parameter to specify the energy of interaction that we take to be between voids and monomers. The partition function for the model is given by

$$Z=\sum\ \kappa^B\eta^{2P}w^{N_c}\lambda^M, \tag{1}$$

where B, M, P and N_c denote the total number of chemical bonds in all polymers, the total number of monomers, the total number of polymers and the total number of nearest-neighbor contacts between voids and monomers, respectively, and $w=\exp(-\beta\varepsilon)$. The sum is over all allowed configurations of the system on the regular lattice. Let N_0 denote the number of voids and N the number of sites on the lattice, such that

$$N=M+N_0. \tag{2a}$$

Moreover, the number of segments in all polymers is

$$N_1=B+P. \tag{2b}$$

Hence, the number of the solvent molecules is

$$N_2=M-N_1=M-B-P \tag{2c}$$

and the problem is uniquely specified. Let us introduce various densities ϕ_0, ϕ_1, ϕ_2 and ϕ_m as the ratios N_0/N, N_1/N, N_2/N and M/N as $N\to\infty$. The bond density $\phi_b=B/N$ and number density $\phi_p=P/N$ are also introduced similarly, such that

$$\phi_1=\phi_b+\phi_p,\quad \phi_m=\phi_1+\phi_2 \tag{3a}$$

and

$$\phi_0+\phi_1+\phi_2=1. \tag{3b}$$

The ratio

$$\bar{N}=\phi_1/\phi_p \tag{4}$$

will be used as the *average degree of polymerization* for polymers.

The physics of the model is easy to predict. Whenever we consider any particular limit for a given activity out of κ, η, λ or the weight w, we do so under the condition that all other *remaining* activities or weight remain *fixed* and *finite*. This is implicitly assumed in the following discussion:

(1) $\lambda\to 0$. There are no monomers in the system and we obtain a pure vacuum state ($\phi_0=1$).
(2) $\lambda\to\infty$. The monomer density $\phi_m\to 1$ and we obtain an *incompressible* system.
(3) $\kappa\to 0$. There can be no polymers and $\phi_1=0$. We have a pure, i.e., compressible ''solvent'' system.
(4) $\kappa\to\infty$. We have a macroscopic polymer covering the entire lattice ($\phi_1=1$). This is known as the Hamilton walk limit, in which a polymer covers every site of the lattice.
(5) $\eta\to 0$. The number density $\phi_p\to 0$. However, ϕ_1 may or may not be zero. If $\phi_1=0$, we would say that there are no polymers in the system. If $\phi_1\neq 0$, we would say that there is a macroscopic polymer that is infinitely long ($\bar{N}\to\infty$).
(6) $\eta\to\infty$. Here, each polymer becomes a dimer and the entire lattice is covered by dimers such that $\phi_p=1/2$ and $\phi_1=1$. This is an incompressible limit of dimers.
(7) $w\to 0$. There is no possibility of contacts between monomers and voids. In other words, either we have a pure vacuum state or a pure state of only monomers (solvents and segments) with coexistence between these two pure states. No phase transitions are possible in the pure vacuum state. However, the pure monomer phase will exhibit the Flory–deGennes (F–dG) transition at $\eta=0$ as κ is increased, see (5) above and below.
(8) $w\to\infty$. There is an infinitely strong ''attraction'' between monomers and voids, such that ϕ_c attains its maximum value. This is a polymer solution in a liquid phase. Again, there would be a F–dG transition at $\eta=0$ as κ is increased.

The limit $\lambda\to\infty$ gives rise to an incompressible system. In this system, there exists a continuous transition, known as a polymerization transition, from no or only small polymers to a macroscopically large polymer at some critical value κ_c as first argued by de Gennes[14] and has been investigated thoroughly by many workers; see for example, Ref. 15. We will term such a critical transition a F–dG polymerization

transition. At the critical transition, the polymer is a fractal object. Near κ_c, $\overline{N}\sim 1/\Delta\kappa$, where $\Delta\kappa=\kappa_c-\kappa\geqslant 0$, and the radius of gyration R is given by

$$R\sim\overline{N}^{\nu},$$

where ν is the Flory exponent ≈ 0.6 in three dimensions.

The F–dG criticality due to polymerization transition disappears as soon as $\eta>0$. This F–dG critical point at $\eta=0$ will turn into a surface of critical points in the four-dimensional κ-η-λ-w phase space and one of our aims is to study how and where this surface appears.

It is clear from the above discussion that we must consider the following three phases in the model: (i) monomer-rich phase which also includes the pure solvent phase, (ii) monomer-poor phase which also includes the pure vacuum state and (iii) the polymerized phase which appears only when $\eta=0$. We will use the abbreviations MR phase, MP phase and P phase to denote the three phases, respectively. At low temperatures, the first two phases represent the liquid and the vapor states of either the pure solvent or the solvent with a small amount of polymers. At high enough temperatures, there is no qualitative distinction between these two phases. We will term this high temperature phase a disordered fluid phase and denote it by D phase. The P phase represents a liquid state (i.e., a solution) of infinitely long polymers that becomes denser as κ increases. It is the possible phase separations among these three phases that is central to this study. These phase transitions enable us to unravel the physics behind the free-volume concept as our comprehensive study will show. For $\eta\neq 0$, there is no distinct P phase, even though there are polymers in the system for all values of κ, no matter how small it is. We may introduce the notion of a polymer-poor (PP) phase and a polymer-rich (PR) phase only for the sake of convenience as the difference between the two is only in the amount of polymers present. Indeed, if there is a phase separation between PP and PR phases, it must eventually end in a critical point above which, there can be no distinction between the two phases. This is similar to the situation between the liquid and vapor phases of a system.

III. MAGNETIC ANALOGY

The compressible polymerization model, as mentioned above, is also convenient for our purpose due to the following two reasons:

(i) The corresponding incompressible version ($\lambda\to\infty$) has been thoroughly investigated in the literature;[14,15]

(ii) the latter model can be mapped onto a p-component magnetic model in the limit $p\to 0$, as first demonstrated by deGennes.[14]

The extension of the incompressible magnetic analogy to the case of compressible polymer solution is trivial if we adopt the standard technique[16] for introducing dilution in simple magnetic systems. One considers a dilute p-vector model by associating a dilution variable $n_i=0,1$ at each site of the lattice such that $n_i=0$ indicates the presence of a void and $n_i=1$ indicates the presence of a monomer.

We will adopt the above extension of the magnetic analogy to analyze our model system in Eq. (1). We introduce two magnetic spins, an Ising spin σ_i or the occupation number n_i

$$\sigma_i=(2n_i-1)=\pm 1;\quad n_i=0,1, \tag{5a}$$

and a p-component spin $\mathbf{S}_i$ that points along the axes of the p-dimensional spin space

$$\mathbf{S}_i=(0,0,\ldots,\pm\sqrt{p},0,\ldots,0), \tag{5b}$$

at each site of the lattice. Each spin $\mathbf{S}_i$ satisfies the constraint $\mathbf{S}_i^2=p$.

We now show that the following reduced Hamiltonian

$$\mathscr{H}=K\sum_{\langle i,j\rangle} n_i\mathbf{S}_i\cdot n_j\mathbf{S}_j+H\sum_i S_i^{(1)}n_i$$

$$+(J/2)\sum_{\langle i,j\rangle}(1-\sigma_i\sigma_j)+H'\sum_i n_i \tag{6}$$

for the magnetic system will describe the compressible polymer solution as $p\to 0$. A factor $(-\beta)$ has been absorbed in $\mathscr{H}$ to make it dimensionless. Apart from the coupling K that is never negative, the other three couplings J, H and H' can be of either sign. The sum over $\langle ij\rangle$ is over distinct nearest-neighbor pairs of sites and the sum over i is over all sites. The ''temperature'' β^{-1} of the magnetic system need not be the same as the real temperature T in the polymer system. However, they can be taken to be the same as we will show below; see the discussion following Eq. (10b). The partition function is now obtained by summing over all distinct spin states of $\{\sigma_i\}$ and $\{\mathbf{S}_i\}$:

$$Z_p=\left(\frac{1}{2p}\right)^N\sum_{\{\sigma_i\}}\sum_{\{\mathbf{S}_i\}}\exp(\mathscr{H}) \tag{7}$$

in which $\mathscr{H}$ is given in Eq. (6). The connection with the polymer problem of interest here is obtained by taking the limit $p\to 0$.

We first consider the case when $n_i=1$ at *all* sites of the lattice. This is the *incompressible* limit of the model; see below also. In this case, the last two terms in Eq. (6) give a constant contribution to $\mathscr{H}$. The first two terms then describe the original model for the magnetic analogy proposed by de Gennes.[14,17] In that model, $K\geqslant 0$ represents a ''ferromagnetic coupling'' between neighboring spins $\mathbf{S}_i$ and H represents a magnetic field which couples to only one of its components, taken to be the $\alpha=1$ here. It is well known[14,17] that in the incompressible limit, the above partition function Z_0, in the limit $p\to 0$, describes a polydisperse solution of linear chains in an athermal solution. The partition function for such an ensemble is given by [see Eq. 10(a) for κ and η]

$$\hat{Z}=\sum\ \kappa^B\eta^{2P},$$

in which κ and η have the same meaning as in Eq. (1). Indeed, the above partition function can be obtained from Eq. (1) by setting $w=1$ and $\lambda\to\infty$, which ensures that $M\to N$. It is easily seen that $\hat{Z}=Z_0/\lambda^N$ in the above limit.

We now turn to the general case of arbitrary n_i. The additional magnetic field H' couples only to n_i and the Ising

interaction strength is $J/2$ with J negative (positive) indicating a ferromagnetic (antiferromagnetic) interaction among the Ising spins. The above Hamiltonian has interesting symmetry properties under the *up–down* transformations:

$$\mathbf{S}_i \to -\mathbf{S}_i, \tag{8a}$$

$$\sigma_i \to -\sigma_i. \tag{8b}$$

Both symmetries are the symmetries of the original Hamiltonian in Eq. (6) for $H=0$ and $H'=0$. This means that the average values of both spins will remain *zero* for $H=H'=0$. We say that the up–down *symmetry* of both kinds of spins is *not* broken. For $H=0$ and $H'\neq 0$, only the first symmetry in Eq. (8a) remains a symmetry for the Hamiltonian. Thus, the average of the p-component spins remains zero, but not of the Ising spins. We say that the up–down symmetry of the Ising spin is broken *explicitly* by its symmetry-breaking field which is not zero anymore, but not of the p-component spins. For $H\neq 0$ but $H'=0$, neither symmetry is a valid symmetry of the Hamiltonian. Thus, the up–down symmetries of both spins are again broken explicitly by their symmetry–breaking fields H and H'. These symmetry considerations are going to be very useful when we study the phase diagram later. There we will discover that the above symmetries can be *spontaneously broken* even if we are in the symmetry space of the Hamiltonian, a well-known fact in phase transitions.

The connection of the above magnetic model, Eq. (7), with the compressible polymer problem is easily established.[18] We adapt the method of Ref. 15(b) to the present case. We must consider $n_i=0$ and $n_i=1$ separately. When we expand the exponential term containing H [see Eq. (5), Ref. 15(b)] for $p\to 0$ we rewrite it as follows:

$$\exp(Hn_iS_i^{(1)}) = (1-n_i) + n_iHS_i^{(1)} + n_i(1+H^2(S_i^{(1)})^2/2).$$

The term linear in H gives rise to an end point of a polymer and the third term contributes

$$z = 1 + H^2/2 \tag{9}$$

at each site occupied by a solvent (a monomer which is not part of a polymer). The first term contributes unity at each site occupied by a void. Since $n_i=1$ at all sites which are covered by polymers, the contribution from a configuration containing P polymers with B total bonds is K^BH^{2P}. In addition, each solvent contributes z. From the H' term, we observe that each monomer contributes $e^{H'}$. Similarly each nearest-neighbor contact between a void and a monomer contributes e^J. Using Eq. (2c) to express N_2 as $M-(B+P)$, we finally find that the partition function can be recast in the form equation (1), provided we make the following identifications:

$$\kappa = K/z, \quad \eta^2 = H^2/z, \quad \lambda = ze^{H'}, \quad w = e^J. \tag{10a}$$

This completes our derivation of the magnetic analogy for the compressible system.

It should be stressed that a negative value of J is needed to produce phase separation. Since a factor of β is already present in the definition of J [see the comments immediately after Eq. (6)], we notice that the F-H chi parameter is given by

$$\chi = -qJ; \tag{10b}$$

the negative sign is to make χ positive in the region where phase separation occurs. From now on, we would only consider $J\leqslant 0$, as it is here that we expect phase separations to occur. However, our theory is equally applicable to the miscible regime $J>0$. The temperature T in the polymer system must be thought of as the inverse of χ. From Eq. (10b), we note that, provided we are restricting ourselves to a negative J as we plan to do, J increases as T increases. Note that this T behaves the same way as the inverse of β that was used in the definition of the magnetic Hamiltonian in Eq. (6). Thus, the temperature of both the systems can be conveniently identified as the same.

Consider a fixed value of H and focus on the three-dimensional phase space K-w-H'. Note that there is no interaction between the solvent and the segments. Hence, no phase separation between them is possible. The monomer–void (liquid–gas) phase separation (with liquid representing a MR phase and gas representing void-rich, i.e., a MP phase) corresponds to the phase separation between oppositely magnetized Ising states. This phase separation ends in a critical point, and is induced by varying H'. This also implies that these transitions belong to the Ising universality class, as expected.

In the incompressible limit ($H'\to\infty$), there is no phase separation of the above kind.[14,15] For $\kappa<<1$, monomers are mostly in the form of the solvent, giving rise to a PP phase. For $\kappa>>1$, most monomers polymerize, thus giving rise to a PR phase. It is possible to have a phase transition between them as κ, i.e., K is increased. In the incompressible limit, this is the continuous F–dG transition provided $H=0$. This transition will persist as free volume is introduced. But the *competition* with the free volume can change this into a discontinuous transition. We will see that this indeed happens. We would, therefore, find it useful to distinguish between the PR phase ($\kappa>>1$) and the PP phase ($\kappa<<1$) in our study, as said earlier. We should again note that, since the difference between the two is only quantitative, the phase separation between them must eventually end in a critical point. Furthermore, at such a phase separation, we will always call one phase to be a PP phase and the other one a PR phase. What we will discover, to our surprise, is that the phase separation ends in two critical points in some cases. These critical points turn into theta points for $H\to 0$.

IV. MEAN-FIELD APPROXIMATION

We now check the above qualitative scenario quantitatively in a mean-field approximation. We extend the method proposed in Ref. 17. We assume $\mathbf{m}$ and n denote the thermodynamic average values of $\mathbf{S}_i$ and n_i, respectively, and introduce their respective fluctuations $\delta\mathbf{S}_i$ and δn_i such that

$$\mathbf{S}_i = \mathbf{m}_i + \delta\mathbf{S}_i, \quad n_i = n + \delta n_i. \tag{11}$$

We substitute these in Eq. (6), and retain terms only up to first order in fluctuations and the cross term $\delta n_i \delta\mathbf{S}_i$. This

approximation amounts to throwing away correlations among fluctuations at *different* sites. As is well known, this approximation is valid provided $q\to\infty$ and $\beta\to 0$ simultaneously such that Kq and Jq remain finite. We assume this in the following as the topology of the phase diagram is not expected to depend on this approximation. We also relabel Kq and Jq in the following as K and J, respectively:

$$Kq\to K,\quad Jq\to J. \tag{12a}$$

With this relabeling, we observe that now

$$\chi=-J. \tag{12b}$$

After some trivial algebra (see Ref. 17), we finally find that

$$\mathscr{H}=Nf+y\Sigma n_i S_i^{(1)}+x\Sigma n_i, \tag{13}$$

where

$$f=-Km^2n^2/2+Jn^2, \tag{14a}$$

$$x=J(1-2n)+H', \tag{14b}$$

$$y=Kmn+H, \tag{14c}$$

and where we have used the fact that **m** points along $\alpha=1$, the direction along which H points and that we have replaced **m** by its magnitude m.

The equilibrium free energy ω_0 defined in the limit $N\to\infty$ as

$$\omega_0=(1/N)\ln Z_0$$

can be shown[13] to be equal to the adimensional pressure $\beta P v_0$ where P is the pressure and v_0 is the volume per cell of the lattice. The last condition also implies that the volume of each monomer and each void is also v_0. The equilibrium values of m and n, as $p\to 0$, are given by extremizing ω_0 with respect to m and n:

$$m=y/z(y), \tag{15a}$$

$$n=z(y)/[z(y)+e^{-x}], \tag{15b}$$

in which we have introduced a new function

$$z(y)=1+y^2/2.$$

The coefficients x and y in Eq. (13) represent ''effective'' or ''mean''-field $H'_{\rm eff}$ and $H_{\rm eff}$ acting on individual spins n_i and $S_i^{(1)}n_i$, as is evident from a comparison with Eq. (6). It is because of this particular significance of the coefficients that the method of approximation derives its name. Furthermore, the neglect of correlation among fluctuations at different sites, as said earlier, can only be substantiated provided the coordination number $q\to\infty$. This neglect of the correlation is what is customarily called the random-mixing approximation. However, this limit must be taken such that the combinations Kq and Jq, [see Eq. (12a)], must remain *fixed* and *finite* so that the free energy can remain *finite*. Thus, the current approximation is the extension of the random-mixing approximation for ''one energy parameter'' to ''two energy parameters;'' one of them (J) is the true energy parameter but the other one (K) is the bond activity in the context of our polymer problem.

We also observe that the two effective fields, x and y, imply that any physical state in the model will be described by a pair (m,n) of the values of m and n that extremize ω_0. We find that it is given by

$$\omega_0=\beta P v_0=f+\ln[1+e^x z(y)]. \tag{16}$$

We find that the bond density, the number density, the monomer density and the contact density (between voids and monomers) are given, respectively, by

$$\phi_b=\kappa\partial\omega_0/\partial\kappa,\quad \phi_p=\eta(\partial\omega_0/\partial\eta)/2,$$
$$\phi_m=\lambda\partial\omega_0/\partial\lambda,\quad \phi_c=\partial\omega_0/\partial J, \tag{17}$$

as is evident from the partition function in Eq. (1).

We find it convenient to introduce a new density

$$r=mn. \tag{18}$$

It is easy to express the above polymer densities in terms of the magnetic densities r and n. Such a connection then allows us to express every polymer quantity in terms of magnetic quantities. We find that[18]

$$\phi_b=Kr^2/2,\quad \phi_p=(H/2)(H\phi_b-H\phi_m+zr),$$
$$\phi_m=n,\quad \phi_c=n(1-n). \tag{19}$$

The segment density ϕ_1 and the solvent density ϕ_2 in terms of ϕ_b and ϕ_p are given in Eq. (3a), and z is given in Eq. (9).

The average degree of polymerization $\overline{N}$ is a measure of the polymer–solvent size disparity, as mentioned earlier. It is a function of the four activities and can be varied by varying the activities. However, it is possible to vary the activities in a way that $\overline{N}$ remains a *constant* in a single phase region. Since the temperature, determined by w, and the pressure, determined by ω_0, usually change when we vary the activities, it is evident that the free volume will also change, even though $\overline{N}$ will not vary. Hence, $\overline{N}$ alone is *not* sufficient to measure the free-volume disparity, as discussed in Sec. I.

The analysis of Eq. (15) is straightforward and standard. Hence, we briefly outline the method of analysis but discuss extensively the results that are of interest. The pertinent details are presented in Ref. 18. The reference is available upon request.

V. PHASE DIAGRAM

A. $H=0$, $H'=0$

To analyze the phase behavior, we first consider the simpler case of $H'=H=0$. From Eq. (15a), we observe that there are three possible solutions:

$$m=0, \tag{20a}$$

$$m=\pm\sqrt{2(Kn-1)}/Kn. \tag{20b}$$

The last two solutions, Eq. (20b), exist provided

$$K\geqslant K_c=1/n. \tag{21}$$

The two signs of m in Eq. (20b) only imply that m takes one of the two values depending on whether $H\to 0^+$ $(m>0)$, or $H\to 0^-$ $(m<0)$. In the following, we would only be interested in the limit $H\to 0^+$ as negative H has *no* physical

significance for the polymer problem because a physical activity must always be non-negative. However, one must *not* overlook the possibility of the two coexisting states with $m>0$ and $m<0$, respectively, in the corresponding magnetic system as their coexistence determines the nature of the transitions as we will see below.

1. $m=0$

We first consider the simplest possible case ($m=0$). In this case, the solution of Eq. (15b) yields

$$n=g(n)\equiv 1/(1+e^{-x}), \tag{22a}$$

of which $n=\frac{1}{2}$ is *always* a solution but two new solutions $n^{+}>1/2$ and $n^{-}<1/2$ appear for $J<-2$.

The physical state (m,n) for $J>-2$ and small K is given by (0,1/2) since $\sigma=1-2n=0$. It has equal amounts of monomers and voids and represents the D phase: It is a state in which neither of the up–down symmetries in Eqs. (8a) and (8b) is broken. The free volume in the D phase is $\phi_0=\frac{1}{2}$ and does not change as the temperature, i.e., J is reduced. For $J<-2$ and small K, the up–down symmetry, Eq. (8b), of only the Ising spins σ_i is broken, but not of the p-vector spin even though $H'=0$. This is an example of the *spontaneous symmetry breaking* and corresponds to the liquid–vapor (L–V) transition MR phase $(0,n^{+})\rightarrow$ MP phase $(0,n^{-})$ in the pure solvent. These two coexisting phases correspond to the magnetic Ising states $\sigma>0$ and $\sigma<0$, respectively. There are more monomers than voids in the liquid state described by n^{+}, with the situation reversed for n^{-}. This discontinuity $\Delta\phi_0$ in their free volumes is responsible for a discontinuous transition between the two states across $H'=0$. At $J=-2$, where $n^{\pm}\rightarrow 1/2$, we have a L–V critical point of the pure solvent that belongs to the Ising universality class. From Eq. (12b), we observe that $\chi=2$ at the critical point which is a well-known result for simple fluids. This particular critical point has turned into a line C_I of critical points for small K at $J=-2$, as shown in Fig. 1.

For J above $J_{\theta u}=-1$ corresponding to $\theta_{U,0}$ in Fig. 1 and small K, we find that $n=\frac{1}{2}$. As K is increased beyond $K_c=1/n=2$, a nonzero solution for m emerges, the up–down symmetry of $\mathbf{S}_i$, Eq. (8a), is broken *spontaneously* and the monomers begin to polymerize. Since $\phi_b>0$ and $\phi_p=0$, we have $\bar{N}\rightarrow\infty$. We obtain a line C of F–dG critical points at $K=K_c=2$; see Fig 1. The free energy along C is[18]

$$\omega=\ln 2+J/4.$$

At K_c, the unpolymerized D phase $(0,\frac{1}{2})$ continuously but *critically* turns into a polymerized liquid state, the P phase. We show, in Fig. 2(a), the normalized segment density

$$\bar{\phi}_1=\phi_1/(1-\phi_0)$$

as a function of K for $J=-0.8$. We see that $\bar{\phi}_1$ varies continuously but with a singularity at $K=2$. However, this is not true for J immediately below $J_{\theta u}=-1$; see Fig. 2(b) where we show $\bar{\phi}_1$ for $J=-1.7$. For $-1>J>-2$, we obtain a L–V transition between the D phase and the P phase with an upward jump discontinuity in m and n across F_0 (see Fig. 1). The P phase is denser than the D phase. This is demonstrated

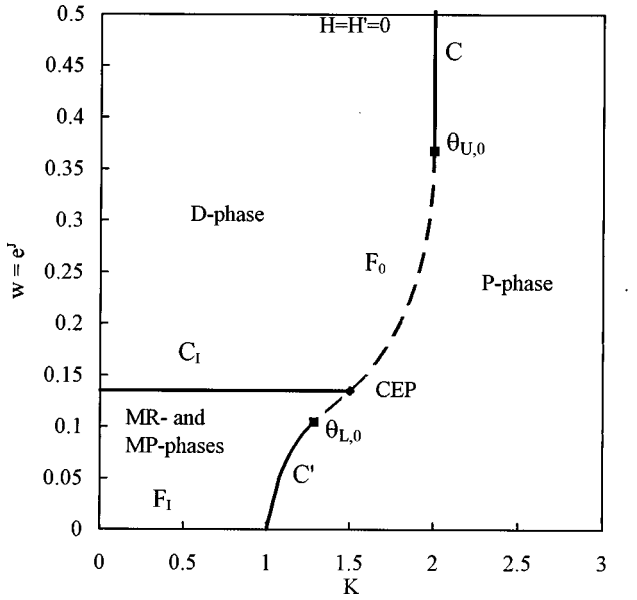

FIG. 1. Phase diagram for the infinitely long polymer, i.e., $H=0$, when $H'=0$ where broken line F_0 represents first-order transitions, continuous lines C and C' represents F–dG continuous transitions, a square represents a tricritical point and a diamond represents a critical end point. The combined curve C' and (CEP, $\theta_{L,0}$) is located at the same place as FF_I of Fig. 3.

below when we consider $m\neq 0$. For $-2>J>J_{\theta L}\cong -2.256$ (see below) where $J_{\theta L}$ corresponds to $\theta_{L,0}$, there is a L–L transition between the MR phase and the P phase across F_0. As the temperature or J is reduced from $J=-2$, the discontinuity in n across F_0 begins to decrease as the MR phase becomes denser faster than the P phase; see the discussion following Eq. (22b). Between $J_{\theta L}$ and $J=-2$, we find that the P phase does not get denser as fast as the MR phase, when the temperature is reduced. This is consistent with the general idea of free-volume effects associated with size disparity.[3–7] Here, we have the extreme case of size disparity as the polymers in the P phase are infinitely large ($\bar{N}\rightarrow\infty$). At $J=J_{\theta L}$, the transition between the MR phase and the P phase turns continuous and gives rise to a line C' of continuous transition. Along C', $K_c=1/n^{+}<2$. Also, there is no discontinuity in the free volumes of the two phases.

The discontinuous L–V transition between the MP phase and the P phase persists all the way down to $J\rightarrow-\infty$. This transition occurs along a curve FF_I that is the union of the portion of F_0 below C_I and C'; see below for more details. The P phase is denser than the MP phase; the difference in the density increases continuously, mostly because the density of the MP phase decreases, as the temperature decreases. Thus, there is no lower temperature at which the transition between the two phases will disappear.

2. $m\neq 0$

We now consider larger values of K where $m\neq 0$. For $m\neq 0$ the above solution, [Eq. (22a)], for n is not valid. The correct solution for n in this case is given by

$$n=h(n)\equiv 1-1/Ke^{x} \tag{22b}$$

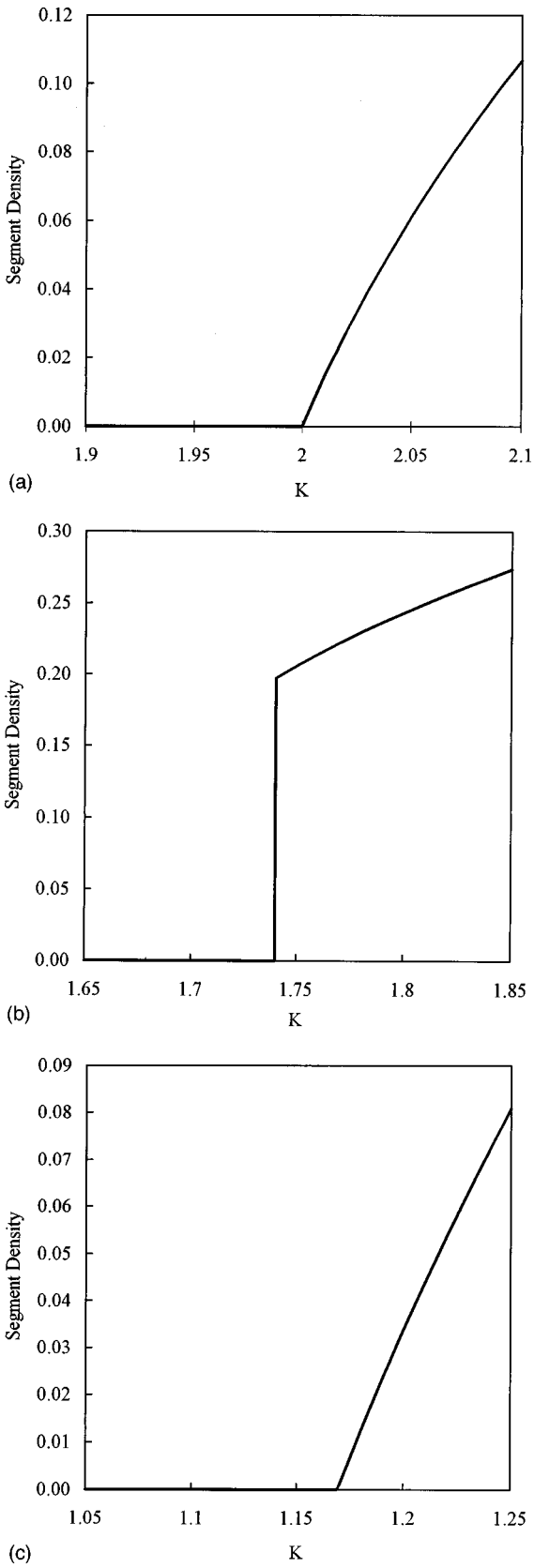

FIG. 2. Segment density profile as a function of K: (a) in the upper continuous transition region with $J=-0.8$, (b) in the first-order transition region with $J=-1.7$, and (c) in the lower continuous transition region with $J=-2.5$.

and represents the P phase. We will use n_g to denote the solution of Eq. (22a) and n_h to denote the solution of Eq. (22b). The solution n_h corresponds to the P phase. Because of the discontinuity in m across F_0, n also undergoes a discontinuous change. For $-2<J<-1$ and $H'\to 0^+$, we find that the stable solution n_h is such that $n_h>n_g=\frac{1}{2}$. At $J\geqslant -1, n_h=n_g$. As J is lowered, n_g remains unchanged but n_h begins to increase and the discontinuity n_h-n_g between the two solutions $n_g=1/2$ and n_h continues to increase along F_0. Thus, the P phase becomes denser, but not the D phase. Below $J=-2$, corresponding to C_I, the solution of Eq. (22a) for the MR phase is given by n_g^+ where n_g^+ is the solution of Eq. (22a) as $H'\to 0^+$. Again, $n_h>n_g^+$. However, as J decreases, n_h keeps increasing but not as fast as n_g^+ which also increases and at $J_{\theta L}$, n_g^+ and n_h *again* become identical and the first-order transition disappears. This proves the statement used above that the MR phase becomes denser faster than the P phase.

For $J<-2$ and $H'\to 0^-$, $n_g^-\leqslant\frac{1}{2}$ for the MP phase, where n_g^- is the solution of Eq. (22a) as $H'\to 0^-$. The two solutions n_h and n_g^- never merge and the first-order transition continues across FF_I down to $J\to-\infty$. Because of the magnetic symmetry about $H=H'=0$, n_g^+ and n_g^- are symmetric about $\frac{1}{2}$, and the free energies of the two solutions are equal. Because of this, the first-order transition curve FF_I (for $H'\to 0^-$) and C' are located at the same place. At $\theta_{L,0}$, the value of J is given by[18]

$$(2J+1)\exp(J+1)=-1. \tag{23}$$

We find numerically that $J_{\theta L}\cong -2.256$, $K_{\theta L}\cong 1.2846$ and $n_{\theta L}={}^1/_{K_{\theta L}}\cong 0.7785$.

We are now in a position to understand the underlying physics of the model in this case. For this, we need to consider all possible solutions for the magnetic system. The disordered D phase corresponds to $J>-2$, $K<2$ and is characterized by the pair $(0,\frac{1}{2})$ for (m,n). As we cross K_c, this phase turns in to a P phase by destroying the up–down symmetry of the **S** spins. Thus, the curve C represents the F–dG polymerization transition. For $K>K_c=2$, there are two coexisting ''magnetic phases'' corresponding to $(\pm m,n)$ and the criticality along C is due to these two phases becoming critical. This criticality is that of the $p=0$ limit of the $O(p)$ model.[14] Note again that we only consider the state with positive magnetization ($H\to 0^+$) as being relevant for the polymer problem as argued above.

Below the critical line C_I which is restricted to $K<2$ in the region where $m=0$, there is a surface F_I of coexistence between the two phases $(0,n^+)$ and $(0,n^-)$ (we suppress the subscript g on n for simplicity) that become critical along C_I. The two coexisting phases are the liquid-like MR phase and the vapor-like MP phase. At $K=K_c$ along C', the two ''magnetized'' phases $(\pm m,n^+)$ emerge, with K_c given by $K_c=1/n^+$ [see Eq. (21)]. For $n=n^-$, we find that there is no real solution of Eq. (20b). Hence, the phase $(0,n^-)$ discontinuously changes into one of the above two ''magnetized'' phases across FF_I. The transition between the MR phase $(0,n^+)$ and the P phase (m,n^+) [or the $(-m,n^+)$] is continuous across C'. This transition is observed at $H'\to 0^+$.

But the transition from $(0,n^-)$ into $(0,n^+)$ or between $(0,n^-)$ and (m,n^+) is discontinuous. At C', we still have the two oppositely ''magnetized'' phases become critical. Hence, C' represents the F–dG transition curve.

At both $\theta_{U,0}$ and $\theta_{L,0}$, there is a line of continuous transitions meeting a line of first-order transitions. Hence, these two points in our model represent *tricritical* points that are also called *theta* points. The lower theta point $\theta_{L,0}$ is evidently associated with the transition between the MR phase and the *P* phase. The *L–V* transitions involving the MP phase remain discontinuous. The point where C_I meets F_0 represents the end of a critical line and is usually called a *critical end point* (CEP).

B. $H=0, H'\neq 0$

Above, we have investigated the possible phase transitions that occur in the symmetry plane $H=H'=0$. We now investigate the possible transitions as H' is varied. The magnetic field H' is the symmetry-breaking field that breaks the Ising symmetry of Eq. (8b) but not the symmetry, [Eq. (8a)], for the *p*-component spins. On the other hand, the F–dG transitions along C and C' are confined in the symmetry subspace $(H=0)$ of the phase space. Since a nonzero H' leaves the symmetry in Eq. (8a) intact, the F–dG transition curves generate a *surface* of these transitions as H' is varied. For $H=0$, $H'\neq 0$, therefore, the two theta points $\theta_{U,0}$ and $\theta_{L,0}$ give rise to two branches θ_U and θ_L given by[18]

$$(2J+1)\exp(J+1-H')=-1, \tag{24a}$$

$$K=2J/(2J+1)=1/n. \tag{24b}$$

The free energy along the two branches is given by

$$\omega=(2J+1)^2/4J+\ln(-2J). \tag{25}$$

The two branches are found to merge together at $\mathcal{T}$, given by $H'\cong 0.193$, and $J=-1.5$. This, in turn, gives rise to a line C_θ of tricritical points, the *projection* of which in the w-H' plane is shown in Fig. 3(a). The lower branch θ_L *exists* only for *positive* H' and abruptly disappears for negative H'.

For $H'\to-\infty$, θ_U occurs at $J=-1/2$. However, we must be somewhat careful as the theta state occurs at a value of K that changes with H'. Hence, we cannot keep K, etc., fixed as $H'\to-\infty$. For finite, but a large negative value of H', there will be a transition from the pure vacuum phase to a *P* phase at some critical value of $K\sim\exp(-H')$. We can formally treat the voids as a new ''solvent'' species, different from the solvent of the homologous species of our original model system. The problem, then, is easily reduced to a problem of a polymer solution and has been investigated thoroughly.[15] We find from Eq. (10a) that $\chi_\theta=\frac{1}{2}$. The graphs of K_θ and $\phi_{m,\theta}=n_\theta$ along C_θ are shown in Figs. 3(b) and 3(c) as a function of J_θ. We note that K_θ is a monotonic increasing function of J_θ. Thus, the values of K_θ on θ_U are higher than its values on θ_L. In particular, $K_\theta\to\infty$ and $J_\theta\to-\frac{1}{2}$ as $H'\to-\infty$. Similarly, $n_\theta\to 0$ in this limit. On the other hand, values of n_θ on θ_U are lower than its values on θ_L. Thus, there is less free volume at θ_L and more at θ_U.

For $H'\neq 0$, the Ising symmetry is *explicitly* broken and the *D* phase is no longer strictly disordered and $n\neq\frac{1}{2}$. For positive H', the stable phase for small K is a MR phase. For negative H', the stable phase for small K is a MP phase.

We now consider what happens as K is increased. For $\lambda>1$ (i.e., $H'>0$), we have a MR phase which supports a

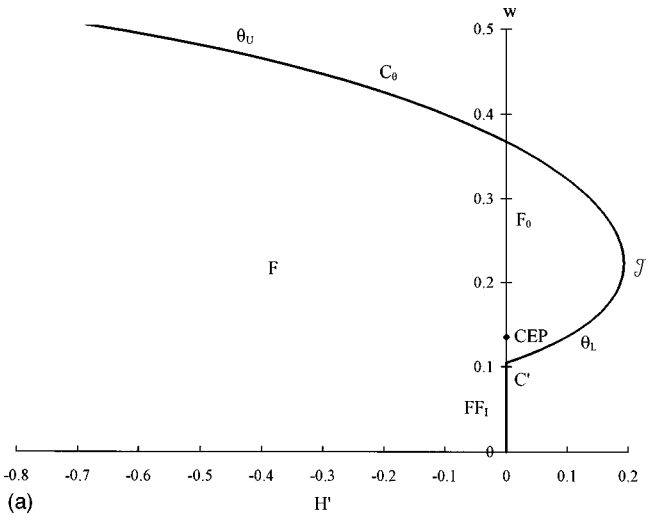

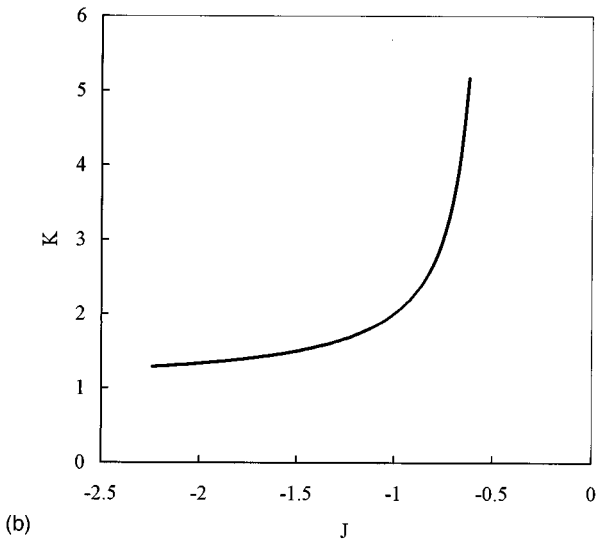

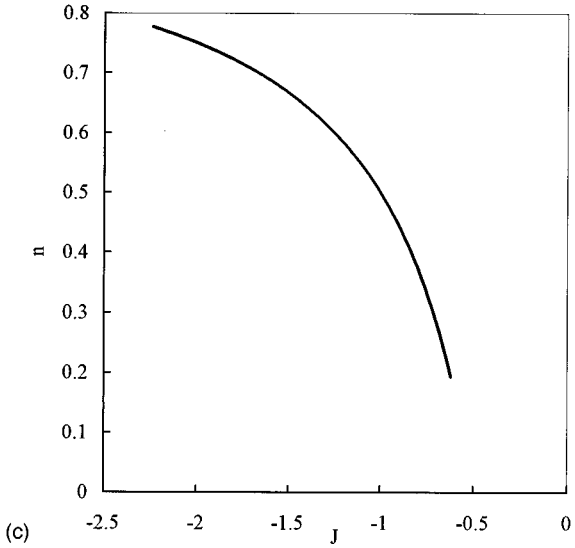

FIG. 3. Line of tricritical or theta points for the polymer solution in (a) w vs H' plane, (b) K vs J plane, and (c) ϕ_m vs J plane.

F–dG transition into a P phase at some critical value of K, as was the case above for $H' \to 0^+$. Hence, there exists a surface in the region to the right of and above C_θ and C' on which these transitions occur. This surface is generated by C and C' of Fig. 1 as H' is varied; see Fig. 3(a) where C_θ and C' form the boundary of this surface. For $H' < 0$ ($\lambda < 1$), we have a MP phase below C_I and a D phase above it, provided K is small. The transition from any of these phases into the P phase occurs across a surface F that lies below and to the left of C_θ and C' [see Fig. 3(a)]. This transition takes place as K is increased and remains discontinuous as was the case above for $H' \to 0^-$ across FF_I. First consider $H' < 0$. Here we obtain transitions from the MP phase or the D phase into the P phase across F. For $H' > 0$, the transition across F is from the MR phase or the D phase into the P phase. The curves F_0 and the portion of FF_I below $\theta_{L,0}$ of Fig. 1 lie in F at $H' \to 0$. The remaining transitions from the MR phase into the P phase are through the F–dG surface.

The critical end point in Fig. 1 is the termination of the line C_I of critical points for the liquid–vapor phase separation of the pure solvent and lies below the turning point $\mathscr{T}$ in Fig. 3(a). It is evident that there is a range of H' over which θ_L can lie above the critical point for the liquid–vapor phase separation of the pure solvent. The critical line C_I and the surface F_I meet the surface F at $H' = 0$. Thus, as argued earlier, there are two surfaces of phase separations in the $H = 0$ subspace. In the four-dimensional parameter space, they would turn into two three-dimensional regions, bounded by two two-dimensional surfaces of critical points.

We consider $H' = 0.03$ and show the C, C' and F_0 in the J-K plane in Fig. 4(a). We show C and F_0 in Fig. 4(b) for $H' = -0.03$. We note that C is also not located at a constant K. In particular, we observe different behavior for C in that C runs towards higher K for $H' > 0$, but towards lower K for $H' < 0$ as J increases. However, the most important feature in Fig. 4(a) is the appearance of the *immiscibility* loop, as shown by the broken curve, while the continuous curves represent C and C'. On the other hand, the continuous transition curve C' has disappeared in Fig. 4(b) for negative H'.

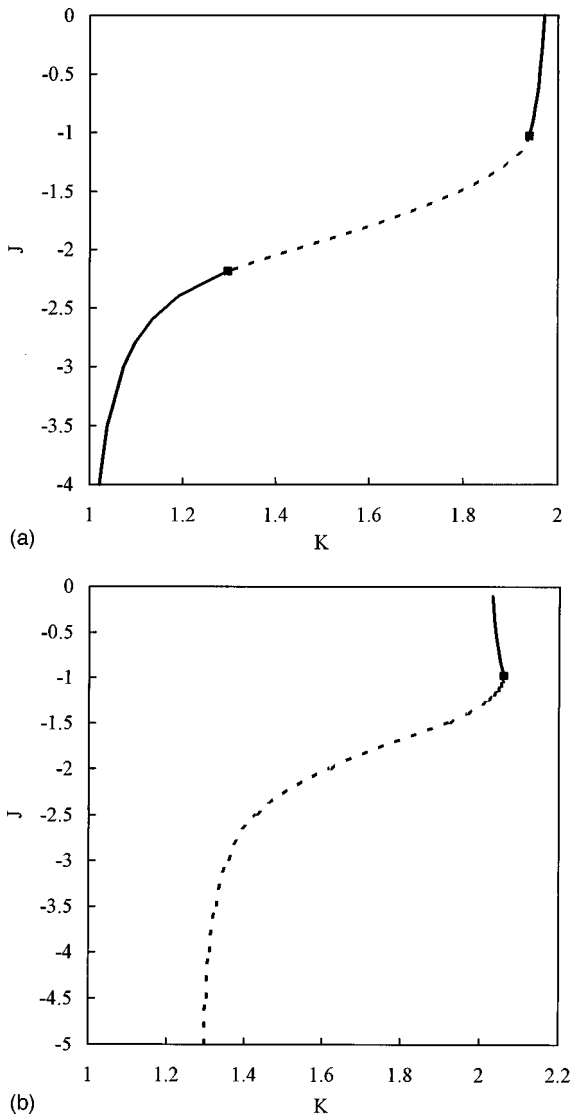

FIG. 4. Phase diagram for infinite polymer in J vs K plane for (a) $H' = 0.03$ and (b) $H' = -0.03$. See Fig. 1 for legends.

C. $H > 0$

For a given $H > 0$, the F–dG surface in Fig. 3(a) *disappears* as the symmetry in Eq. (8a) is explicitly broken and the *tricritical* line C_θ turns into a line C_0 of critical points bounding a surface of first-order transitions similar to F in Fig. 3(a). The lower branch of C_0 now gives rise to a LCST and the upper branch gives rise to an UCST with an *immiscibility loop* in between. For a nonzero H, there is *no* polymerized phase. For $J < -2$, we only have a MR phase for $H' > 0$ or a MP phase for $H' < 0$. Both these phases are rich in polymers (PR phase) for large K but poor in polymers (PP phase) for small K. Since a nonzero H breaks both symmetries, even if $H' = 0$, the Ising critical line C_I, which was confined to $H' = 0$ for $H = 0$ moves to nonzero H, generates a surface as H is varied but this surface is *no* longer confined to $H' = 0$. For this reason, the Ising CEP continues to exist and yields a line of Ising CEPs. Similarly, the phase separation surface F_I of Fig. 1 continues to exist and moves along with C_I. All phase transitions are now between MP, MR and PR phases.

For small K, the first-order transitions across F_I between a MP phase and a MR phase now are restricted to occur at negative H' as a non-zero H enhances the ability for the system to have more monomers. This is shown in Figs. 5(a)–5(c) for two different values of $K = 1.0$ and 1.2. We fix $H = 0.01$. The top of the coexistence curves denotes the L–V critical points that correspond to C_I for nonzero H. We do not observe any appreciable variation in the value of $J(\approx -2)$ at the critical points. In Fig. 5(a), we show the coexistence curve in the J-H' plane for the two values of K. From this we conclude that F_I shifts towards more negative H' as K increases. Thus, FF_I moves to more negative values of H' than any other part of F_I. Indeed, F_I at $K = 0$ must be strictly at $H' = 0$ for all values of H for the following simple reason. At $K = 0$, the bond activity is zero and there can be *no* polymers [except when $\eta \to \infty$ which is impossible in our

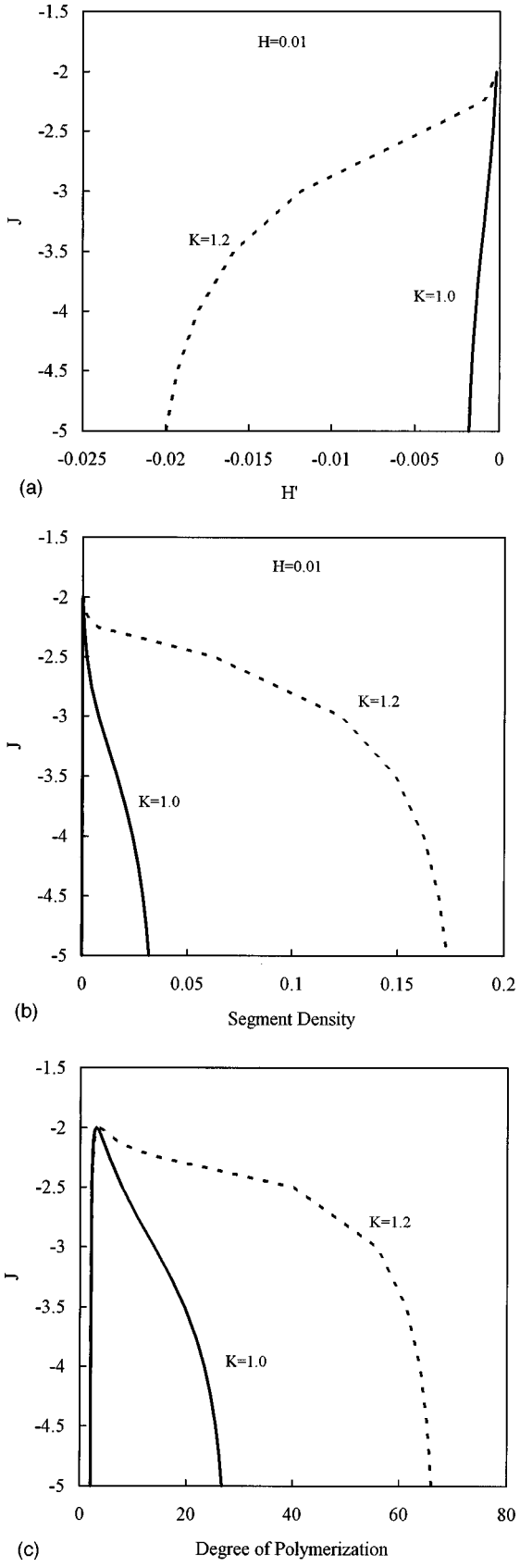

FIG. 5. Phase transition in H' direction for a fixed $H=0.01$: (a) J vs $\overline{\phi}_1$, (b) J vs H', and (c) J vs N.

model since the maximum η is $\sqrt{2}$, see Eq. (10a)] in the system. We have a phase separation in pure solvent and this must be strictly at $H'=0$. In Fig. 5(b), we show the discontinuities in the segment density $\overline{\phi}_1$. The smaller $\overline{\phi}_1 \approx 0$ for both values of K and for all temperatures below the critical temperature. The corresponding phase is a PP phase. The higher $\overline{\phi}_1$ phase represents a PR phase and will have $\overline{\phi}_1$ that would evidently be larger for larger K, as we see from Fig. 5(b). Thus, the discontinuity becomes larger as K increases. In Fig 5(c), we show the discontinuities in $\overline{N}$, the degree of polymerization. Again, its smaller value does not depend on K; only its higher value depends strongly on K. The value of $\overline{N}$ in the PP phase is also insensitive to the temperature and is about 2–3. In the PR phase, it depends strongly on the temperature and can reach to over 25 for $K=1.0$ and 65 for $K=1.2$.

The critical curve C_0 terminates on F_I. It is evident from the way C_θ appears in Fig. 3(a) that C_0 will have a region over which the LCSTs would be *higher* than the Ising (C_I) critical temperatures. The latter correspond to the critical points for a liquid–gas transition for the more volatile system. Indeed, as we see below [see Fig. 6(a)], the LCST ($J \approx -1.98$) for $H=0.01$ and $H'=0.03$ is *higher* than $J=-2$. This should be *contrasted* with the conventional wisdom that LCST's are normally observed 10%–30% below the critical temperature of the pure solvent. The presence of an UCST also *demonstrates* that there is *no* relevance of the *unphysical* singularity due to any *spinodal*.

Since there is no F–dG transition any more, the critical curve C' of Fig. 3(a) has disappeared. The discontinuous transitions between MP and PR phases for negative H' and between MR and PR phases for positive H' are observed across some surface F, similar to that in Fig. 3(a). For a given $H \neq 0$, this surface is bounded by curves FF_I and C_I. This curve FF_I is where the two surfaces F and F_I meet, as was the case for $H=0$ in Figs. 1 and 3(a). The lower branch of C_0, not shown in Fig. 5(a), appears abruptly from FF_I as H' increases. The point at which C_0 ends on F_I is a *new* critical end point.

The immiscibility loop appears when a MR phase makes a L–L transition into a PR phase as J is raised. At the UCST and the LCST, there is *no* difference in the free volumes of the two phases but their difference $\Delta\phi_0$ first begins to increase as J is increased above the LCST, then begins to decrease and eventually vanishes at the UCST, as was discussed earlier for $H=0$. In Figs. 6(a)–6(d), we show the results for $H=0.01$ and $H'=0.03$. In Fig 6(a), we show the immiscibility loop in the J vs ϕ_m plane. In Fig. 6(b), we show the immiscibility loop in the J vs $\overline{\phi}_1$ plane. We show the discontinuities in $\overline{N}$ in Fig. 6(c). In Fig. 6(d), we show the value of J and K for the immiscibility loop. At low temperatures, the discontinuities are larger, the larger the magnitude ($-H'$). However, near $J=-2$, the situation is different. Here, the discontinuities *abruptly* decrease for $H' \cong 0$. The thermal expansion coefficient of the vapor MPphase becomes very small; see the curve in Fig. 6(a) for $H'=-0.001$. Similarly, the expansion coefficient for the PR phase is also very small. We clearly see that the segment

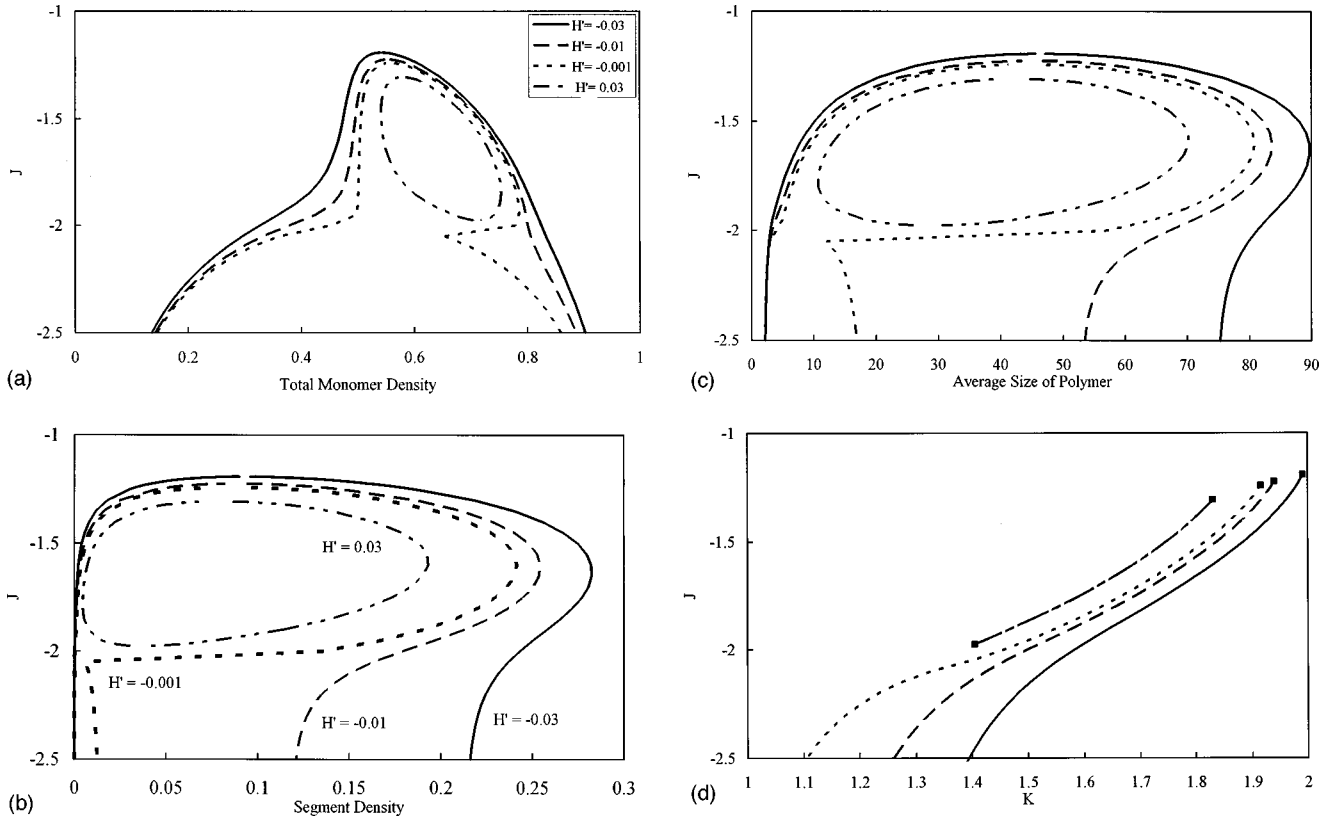

FIG. 6. Consolidated phase diagram: (a) J vs ϕ_m, (b) J vs $\overline{\phi}_1$, (c) J vs $\overline{N}$, and (d) J vs K. See (a) for legends.

density $\overline{\phi}_1$, the monomer density ϕ_m and $\overline{N}$ all show features similar to the free volume in the mixture. The critical value of $\overline{\phi}_1$ is about 0.03 at the LCST and is about 0.07 at the UCST. Note that the critical compositions at UCST and LCST are different. The value for J is about (-1.98) at the LCST and is about (-1.32) at the UCST. The maximum discontinuity in $\overline{\phi}_1$ occurs near $J \cong -1.6$, the discontinuity becoming smaller on either side of this J.

1. Disappearing of immiscibility loop

The immiscibility loop disappears for negative values of H'. This is consistent with our investigation for $H=0$, where we have observed that the immiscibility loop appears only for positive H'. This is clearly seen from Figs. 6(a)–6(d) where we show the coexisting regions in four different planes. The interesting feature we observe is that the maximum discontinuity in $\overline{\phi}_1$ decreases rapidly as H' increases. Therefore, it is not surprising that the LCST *disappears* above some H' at which the turning point similar to $\mathscr{T}$ in Fig. 3(a) occurs.

The surprising feature emerges when we consider what happens when H' is reduced. We see that there are no immiscibility loops for $H'=-0.001$, -0.01 and -0.1. This also implies that a *small* change in H' can abruptly cause LCST to disappear. This is quite remarkable, since the LCST disappears not because the immiscibility loop shrinks in size but because the free volume has increased above a certain critical value.

This raises the question of what happens to the immiscibility loop as H increases. We find a similar behavior in that, for some large H, the immiscibility loop *disappears*. For example, for $H'=0.03$, this happens at $H \geqslant 0.031$, at which the degree of polymerization is $\overline{N}_0 \cong 15$. Since $\overline{N}$ increases as H decreases, the immiscibility loop is present only for $\overline{N} \geqslant \overline{N}_0$. A certain *critical* value of *size disparity* is needed to observe the phenomenon. If the size disparity is less than this critical value, there will not be any phenomenon associated with LCST. Thus, for the ''athermal'' case considered here, we will not observe LCST if we had only small polymers. This is consistent with the expectation that no LCST would be observed for a symmetric blend even if interaction is present. Only an UCST would be observed in this case.

It is clear that the critical value $\overline{N}_0\,(H, H')$ is a function of H and H' both. For a fixed H', there is a certain critical value H_0 of H, which, in turn, determines the critical size disparity $\overline{N}_0$. Alternatively, for a fixed H, there exists a maximum value H_0' of H' above which there would be no LCST phenomenon observed. Since H' controls the monomer density, which in turn determines the free volume, i.e., pressure, we conclude that there exists a maximum pressure above which no LCST would be observed.

To see this most clearly, we plot $\beta P_\theta v_0$ vs J_θ along the tricritical line C_θ in Fig. 7. For $H \neq 0$, the curve relating P_C and J_C along C_0 appears similar to that in Fig. 7 and shows the existence of LCSTs, but only over a finite range of the pressure between P_M and P_L, where $P_M > P_L$. For P

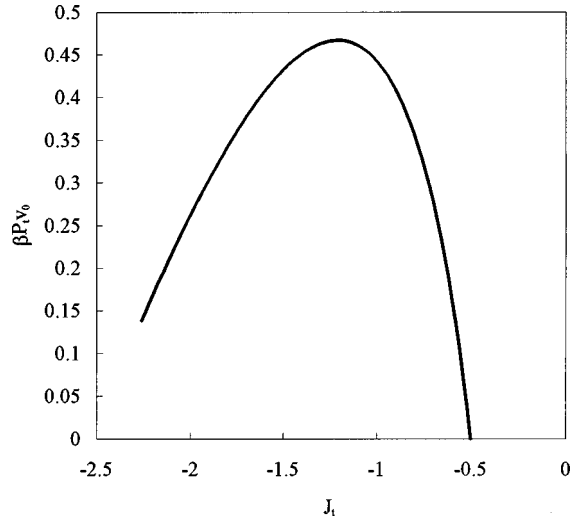

FIG. 7. Reduced pressure $\beta P v_0$ vs J_θ along C_θ.

$<P_L$, only UCST is observed; for $P>P_M$, no phase separation occurs.

2. Appearance of hourglass effect

In Figs. 6(a)–6(d), we have fixed $H=0.01$ and show the coexistence region for different values of H' that clearly show the ''hourglass'' effect emerging. For $H'=0.03$, we only see an immiscibility loop. As mentioned previously, the discontinuities in ϕ_m, $\bar{\phi}_1$ and $\bar{N}$ decrease as H' increases and eventually vanish at its critical value H_0'. Thus, we must consider lower values of H' where the discontinuities are larger. These discontinuities may then be coupled with transitions at lower temperatures to possibly give rise to the hourglass effect.

The transitions at lower temperatures are between the MP and either the MR phase or the PR phase. We first consider the region of H' where the transition between the MP and MR phases is observed. There is now a competition between the LCST at positive H' and these transitions across F. We clearly see the hourglass effect for $H'=-0.001$, -0.01 and -0.03 where no LCST exists. The larger discontinuities are the consequence of the immisciblity loop and are responsible for the bottleneck effect. As H' decreases, the narrow neck widens and eventually destroys the hourglass effect. In this region of H', the transition is between MP and PR phases. Thus, the hourglass effect is *absent* both at high and low values of H'.

Note that the hourglass effect has emerged not because the LCST has ''swallowed'' the UCST for the MP phase→MR phase transition or that the UCST has disappeared. Neither is true. Both are still present in the phase space and the UCST is at a *higher* temperature than the LCST. It is not appropriate to think that both critical points have disappeared. What has happened is this: The plane defined by the fixed values of H and H' crosses the phase diagram in such a way that both critical points are avoided. However, the pattern is obvious. As H' moves towards zero from the negative side, the part of the coexistence region reminiscent of the immiscibility loop appears to be on the verge of being cutoff from the rest of the region to give rise to *two* distinct coexistence regions. That this indeed happens is clearly shown in Figs. 8(a) and 8(b) in which $H'=-0.0001$. In Fig. 8(a), we show the coexistence region in the J-ϕ_m plane where we see two distinct and separate parts, with the immiscibility loop showing a smaller discontinuity than the discontinuity in the lower coexistence region. Moreover, the lower UCST is higher than the LCST, yet the LCST has *not* swallowed the UCST. The upper UCST and the LCST occur at *different* compositions. We show the same coexistence region in the J-$\bar{\phi}_1$ plane where again we have two separate parts. As H' is reduced slightly, the two parts merge and give rise to a phase diagram in the shape of a golf club. The interesting observation is that the critical monomer concentrations at both UCSTs are almost *identical* and about $\frac{1}{2}$.

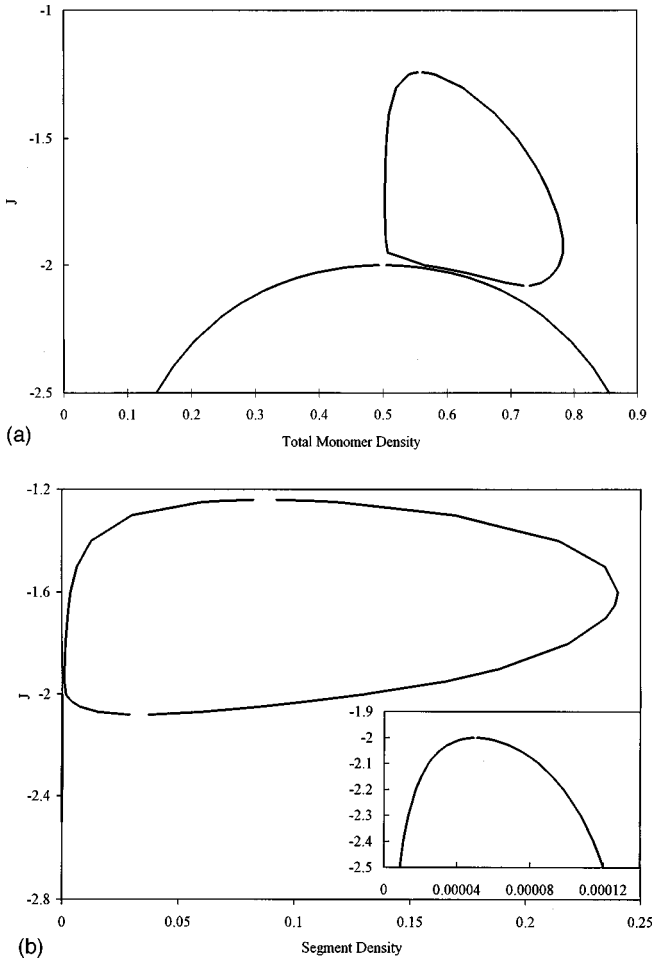

FIG. 8. The coexistence region for $H'=-0.0001$ and $H=0.01$: (a) J vs ϕ_m and (b) J vs $\bar{\phi}_1$. The inset in (b) shows an expanded version of the liquid–vapor phase transition at low temperatures.

Note the new mechanism by which the ''hourglass'' effect has emerged. It is present since we are close to the abrupt emergence of a LCST and, hence, of an immiscibility loop. The latter requires a large discontinuity near the middle of the loop and a vanishing discontinuity at LCST. To be able to accommodate this possibility, the hourglass effect emerges for negative H'.

VI. CONCLUSIONS AND SUMMARY

In order to investigate only the effect of size disparity on the free volume, we have considered a very simple model system that is customarily considered an *athermal* system. Nevertheless, the system is not truly athermal, as was demonstrated in Sec. II. The simplicity of the model was designed to enable us to analytically determine not only the phase diagram, but also demonstrate the usefulness of the volume-expansion coefficient in understanding aspects of a system responsible for producing a LCST. In the process, we were able to show that many of the notions based on our current understanding of the free volume could not be substantiated.

For the benefit of the reader who skipped Secs. IV and V, we provide below a succinct summary of the results. The model system we consider is an equilibrium polymerization model in which compressibility is introduced by incorporating voids as the third component. The model is then related to a *spin system* containing two different kinds of spins. One kind of spin is an Ising spin and the other is a *p*-vector spin. The Ising spin part of the model allows us to describe various liquid–liquid and liquid–vapor phase separations. The *p*-vector spin part of the model allows us to describe equilibrium polymerization, as originally proposed by de Gennes.[14,15] Since no activity is allowed to control the density ϕ_0 of voids or the free volume, the voids play the role of a *reference species* (see Ref. 13 for further details). Accordingly, the free energy corresponding to the partition function in Eq. (1) represents the adimensional pressure $\beta P v_0$ and is given in Eq. (16) in terms of magnetic variables. This derivation is based on a mean-field approximation as described in Sec. IV. The approximation is valid in the limit $q\to\infty$, while keeping the two parameters in Eq. (12a) fixed.

We have obtained the entire phase diagram in the above approximation. Because of the presence of the two symmetry-breaking fields H and H', we must carefully distinguish between the four phases that occur in the symmetry space $H=H'=0$: a *D* phase, a MR phase, a MP phase and a *P* phase. The *D* phase exists only at high temperatures and represents a disordered fluid phase of the pure solvent. For $H=H'=0$, it is a phase in which the monomer fraction is half, the monomers being unpolymerized. As the bond activity $\kappa=K$ increases, the *D* phase critically but continuously goes into a *P* phase. Instead of increasing κ, if we decrease the temperature, the *D* phase undergoes phase separation into two phases: a MP phase and a MR phase. They represent the liquid and the vapor phases of the pure solvent and coexist on a surface F_I of first-order transitions that is located at $H'=0$ ($\lambda=1$). For $H'>0$ ($\lambda>1$), the MR phase is stable. For $H'<0$ ($\lambda<1$), the MP phase is stable. The surface terminates in a line C_I of critical points; the latter is located at $J=-2$ and small K. The MR phase undergoes a critical F–dG transition into the *P* phase at some $K=K_c$. The free volumes of the two phases are the same at the transition and so are the sizes of the polymers ($\bar{N}\to\infty$). What is interesting and surprising is that, as the temperature is raised, nothing changes for a while as long as we are below $\theta_{L,0}$. The free volume continues to increase. However, above $\theta_{L,0}$, the free volume of the MR phase suddenly begins to increase faster than the free volume of the *P* phase and the transition between them becomes discontinuous and gives rise to a nonzero discontinuity $\Delta\phi_0$ between the coexisting phases. This difference in the free volume continues to increase for a while as the temperature rises. As the temperature rises further, $\Delta\phi_0$ begins to decrease until eventually it vanishes at $\theta_{U,0}$ and remains zero above it. This change in the behavior of $\Delta\phi_0$ is due to the difference in the *volume expansion* coefficients of the two phases. In the liquid phase, below C_I, the pure solvent, i.e., the MR phase, expands at a faster rate than the liquid *P* phase. Above C_I, the MR phase and the MP phase become one (the *D* phase). This phase has a *zero* expansion coefficient, but the *P* phase continues to expand until we reach $\theta_{U,0}$ where $\Delta\phi_0$ vanishes.

The discontinuous transition above C_I occurs across F_0. The new feature we have discovered is that the lower theta point occurs in the MR phase which is a liquid phase of the pure solvent. Hence, it is the *liquid phase* that *supports* the lower theta point. The vapor phase, i.e., the MP phase does not support a lower theta point. At $T=0$, the vapor phase is a pure vacuum ($n=0$). There is a first-order transition from the vacuum to a *P* phase in which the free volume is zero. Thus, $\Delta\phi_0$ has its maximum value at $T=0$. As T rises, the free volume in the MP phase begins to decrease but that in the *P* phase begins to increase. As a result, $\Delta\phi_0$ begins to decrease until finally, it vanishes at $\theta_{U,0}$. We have shown that θ_U lies below $\chi_\theta=\frac{1}{2}$. Thus, the transitions corresponding to these θ_U's should be *experimentally* observable.

For $H'\neq 0$, but for $H=0$, the situation does not change. The MP phase, confined to $H'<0$, continues to support only an upper theta state. The MR phase, confined to $H'>0$, is the one that continues to support both a lower theta state and an upper theta state. Furthermore, as H' increases, the free volume of the MR phase begins to decrease. Thus, as the MR phase becomes denser and denser, the ability for the liquid solvent to expand becomes limited and eventually, the lower theta point disappears at $\mathscr{T}$. As H' increases, there is a range of H' over which the lower theta states lie above C_I. Thus, there is *no* thermodynamic argument to suggest that the lower theta point (or LCST for finite polymers) must always lie below the critical point for the pure solvent.

From the topology of Fig. 3(a), we conclude the following. There is a surface *F* across which the transition to the *P* phase from any one of the MP, *D* or MR phases is discontinuous. The surface is bounded by a line of theta points which separates it from a surface of the F–dG transition. There is another surface F_I at low J bounded by C_I at $J=-2$ which comes and hits *F* along a curve FF_I that lies in the $H'=0$ plane in the $H=0$ three-dimensional w-H'-K subspace.

For $H>0$, the situation is similar to the above, except that the F–dG surface and C' disappear. The line of theta points turn into a line C_0 of continuous transitions, giving rise to LCST and UCST. The surface F_I continues to persist along with its boundary C_I. This surface hits *F* along FF_I on which C_0 ends. The only difference is that F_I is no longer restricted to $H'=0$, except at $K=0$. As K increases, F_I bends more and more towards negative H'. Otherwise, all

features of Fig. 3(a) persist. The point where C_I meets F and the point where C_0 meets F_I are two distinct critical end points, one for each phase separation. Moreover, FF_I is a line of triple points.

In the full four-dimensional phase space, C_0 forms a critical surface. Over a finite region of H and H', this surface contains a bent region corresponding to the immiscibility loop. The symmetry $H \to -H$, $\mathbf{S}_i \to -\mathbf{S}_i$ ensures that there exists another critical surface obtained by its image in the $H=0$ plane. These two critical surfaces meet with the deGennes–Flory critical surface along C_θ. By definition, then, C_θ is the line of tricritical points that, as deGennes[14] has argued earlier in a different context, represent theta states.

It is interesting to move around in the full four-dimensional phase space along paths that correspond to T increasing monotonically, but not necessarily along fixed H and H'. In this case, it is possible to cross the critical surfaces formed by C_0 and C_I in a variety of ways, thus giving rise to a variety of phase diagrams. For example, we can take a path that crosses only C_0 but not C_I at two points so that both points lie on the portion of the surface formed by what we have termed UCST in the earlier discussion. Yet, one of the two points will give a LCST and the other an UCST. Thus, to some degree, the *distinction* between the UCST and LCST is somewhat *arbitrary* and depends on the path taken in the phase space. Similarly, the path may cross both surfaces and the phase diagram will be distinct with the previous case. It is also clear, as was mentioned earlier, that a slight change in the way the path crosses the phase space can make a LCST appear or disappear.

We can consider crossing the critical phase separation region along a path which crosses the critical surface at two points, again giving rise to an UCST and a LCST. In this case, one obtains an immiscibility loop. We expect a similar behavior even when we have a monodisperse solution, provided we overlook the difference in the average polymerization index in the coexisting phases. We should add at this point that while we have studied a polydisperse system, we do not expect polydispersity to change the generic features of the phase diagram. In particular, we believe that the theta line C_θ is not affected by the presence of polydispersity. Furthermore, we have recently shown[13] that the equation of state on a Bethe lattice does not depend on the presence of polydispersity. Thus, we believe the topology of the phase diagram to be generic.

We are now in a position to summarize our conclusions regarding the five features based on the current but an incomplete picture that were mentioned in Sec I.

(i) The phenomenon of LCST exists only when the size disparity measured by $\overline{N}$ is larger than some critical value $\overline{N}_0$. The critical size depends on the pressure and the composition. For $\overline{N} < \overline{N}_0$, the phenomenon does not exist.

(ii) The phenomenon of LCST exists only in a finite pressure range (P_L, P_M) where $P_M > P_L$. Too much of free volume or too little of it destroys the phenomenon. In particular, a slight change in the free volume near the lower pressure can make LCST abruptly disappear. Near P_M, the disappearance of LCST is gradual as the immiscibility loop disappears gradually.

(iii) There are two kinds of UCSTs in the model system. The UCST at lower temperatures is for the more volatile component and the upper UCST is for a transition into a PR phase.

(iv) It is possible for the LCST to be higher than the lower UCST.

(v) There are many possible phase diagrams including only an immiscibility loop, an immiscibility loop in conjunction with an immiscibility region with an UCST, and an immiscibility region in the shape of a golf club or an hourglass.

In conclusion, we have presented a simple theory that allows us to describe free-volume effects finally in a quantitative form. The model system was intentionally chosen to be a very simple system, traditionally known as an *athermal* system, for the basic reason that it allows us to probe only the effects produced by size disparity. The model describes an equilibrium polymerization process. Because the unreacted monomers and reacted monomers are homologous species, they have *no* effective interaction. We treat the unreacted monomers as the solvent. The presence of free volume is described by allowing voids in the model. Because of the presence of voids, the model is *not* truly athermal as was argued here. This fact is not widely appreciated. According to the conventional wisdom, such a model system is not expected to exhibit any UCST. We demonstrate, however, that there are *two* different kinds of UCSTs, each describing liquid–vapor transitions. One of them represents the transition in a system containing mostly the smaller component, i.e., the solvent. The other one represents the transition in a system containing polymers. In the limit when there is *no* solvent in the mixture, we have shown that the latter UCST is given by $\chi_\theta = 1/2$ that is identical in value to the chi parameter at the theta point for a polymer solution. This should not be surprising as we can always treat the void as a solvent in our lattice model. This also shows that all UCSTs we have in our model are at temperatures that are realistic from an experimental point of view. In particular, if there is interaction between the solvent and the segment, we would expect the UCST for the corresponding phase separation to be in a similar range of the appropriate chi parameter. The study dispels some of the misconceptions related to free volume. A very clear understanding has emerged for the rich topology of the phase diagram that includes an hourglass effect or a golf club effect which are found in the model. Thus, the work provides a leap in our understanding of those features of the free-volume effects that are induced by size disparity. It would be interesting to fully investigate the effects of the interaction between the segment and the solvent. This is a project for the future. We have also studied the effects of special, i.e., directional interactions using a similar model. The results will be presented separately.

[1] *Polymer Compatibility and Incompatibility: Principles and Practices*, edited by K. Sole, MMI Press Symposium Series 2 (Harwood, New York, 1982).
[2] P. I. Freeman and J. S. Rowlinson, Polymer **1**, 20 (1960).
[3] V. Mathot, Comptes Rendus Reunion Sur les Changements de Phases, Paris, France, 1952, p. 115.
[4] I. Prigogine, N. Trappeniers, and V. Mathot, Discuss. Faraday Soc. **15**, 93 (1953).
[5] I. Prigogine, V. Mathot, and A. Bellemans, *The Molecular Theory of Solutions* (North-Holland, Amsterdam, 1957).
[6] P. J. Flory, J. L. Ellenson, and B. E. Eichinger, Macromolecules **1**, 279 (1968).
[7] D. Patterson, Macromolecules **2**, 672 (1969).
[8] R. H. Lacombe and I. C. Sanchez, J. Phys. Chem. **80**, 2568 (1976).
[9] *Models for Thermodynamic and Phase Equilibria Calculations*, edited by S. I. Sandler (Marcel Dekker, New York, 1993).
[10] A. Sariban and K. Binder, Macromolecules **21**, 711 (1988).
[11] (a) H Erying, J. Chem. Phys. **4**, 283 (1926); (b) T. D. Lee and C. N. Yang, Phys. Rev. **87**, 404 (1952).
[12] J.-H. Ryu and P. D. Gujrati, J. Chem. Phys. **107**, 3954 (1997).
[13] P. D. Gujrati, J. Chem. Phys. **108**, 6952 (1998).
[14] P. G. deGennes, *Scaling Concepts in Polymers Physics* (Cornell University Press, Ithaca, NY, 1979).
[15] (a) P. D. Gujrati, Phys. Rev. B **24**, 2854 (1981); (b) Phys. Rev. A **24**, 2096 (1981).
[16] E. K. Riedel and F. J. Wagner, Phys. Rev. Lett. **29**, 349 (1972).
[17] P. D. Gujrati, Phys. Rev. B **25**, 3381 (1982).
[18] Mukesh K. Chhajer, Ph.D. dissertation, The University of Akron, 1998.